Current Biology *18*, 1600–1605, October 28, 2008 ©2008 Elsevier Ltd All rights reserved DOI 10.1016/j.cub.2008.08.073

Report

An Expanded Biological Repertoire for Ins(3,4,5,6)P_4 through its Modulation of ClC-3 Function

Jennifer Mitchell,[1] Xueqing Wang,[2] Guangping Zhang,[2] Martina Gentzsch,[3] Deborah J. Nelson,[2] and Stephen B. Shears[1,*]
[1]Inositol Signaling Group
National Institute of Environmental Health Sciences
National Institutes of Health
U.S. Department of Health and Human Services
P.O. Box 12233
Research Triangle Park, North Carolina 27709
[2]Department of Neurobiology, Pharmacology and Physiology
The University of Chicago
Chicago, Illinois 60637
[3]Department of Cell and Developmental Biology
and Cystic Fibrosis Research Center
University of North Carolina
Chapel Hill, North Carolina 27599

Summary

Ins(3,4,5,6)P_4 inhibits plasma membrane Cl^- flux in secretory epithelia [1]. However, in most other mammalian cells, receptor-dependent elevation of Ins(3,4,5,6)P_4 levels is an "orphan" response that lacks biological significance [2]. We set out to identify Cl^- channel(s) and/or transporter(s) that are regulated by Ins(3,4,5,6)P_4 in vivo. Several candidates [3–5] were excluded through biophysical criteria, electrophysiological analysis, and confocal immunofluorescence microscopy. Then, we heterologously expressed ClC-3 in the plasma membrane of HEK293-tsA201 cells; whole-cell patch-clamp analysis showed Ins(3,4,5,6)P_4 to inhibit Cl^- conductance through ClC-3. Next, we heterologously expressed ClC-3 in the early endosomal compartment of BHK cells; by fluorescence ratio imaging of endocytosed FITC-transferrin, we recorded intra-endosomal pH, an in situ biosensor for Cl^- flux across endosomal membranes [6]. A cell-permeant, bioactivatable Ins(3,4,5,6)P_4 analog elevated endosomal pH from 6.1 to 6.6, reflecting inhibition of ClC-3. Finally, Ins(3,4,5,6)P_4 inhibited endogenous ClC-3 conductance in postsynaptic membranes of neonatal hippocampal neurones. Among other ClC-3 functions that could be regulated by Ins(3,4,5,6)P_4 are tumor cell migration [7], apoptosis [8], and inflammatory responses [9]. Ins(3,4,5,6)P_4 is a ubiquitous cellular signal with diverse biological actions.

Results and Discussion

ITPK1 is a multifunctional kinase and phosphotransferase that interconverts Ins(3,4,5,6)P_4 with Ins(1,3,4,5,6)P_5 [10]. The poise of this substrate cycle becomes weighted in favor of Ins(3,4,5,6)P_4 accumulation whenever phospholipase C is receptor-activated [10, 11]. Intracellular [Ins(3,4,5,6)P_4] rises from 1 μM in resting cells up to 10 μM after receptor activation [11]. In epithelial cells, elevated [Ins(3,4,5,6)P_4] inhibits Ca^{2+}-activated Cl^- efflux [1, 12–14]. However, no one has established the molecular identity of any Cl^- channel (or transporter) that is regulated by Ins(3,4,5,6)P_4 in vivo. For several years, the usual suspects that have been rounded up in literature reviews [3–5] have fallen into three separate families: CLCA, bestrophin, and ClC. We exclude the CLCA family because its pharmacological properties (inhibition by dithiothreitol [15]) and electrophysiological parameters (13–30 pS unitary conductance [15]) do not match those of the Ins(3,4,5,6)P_4-inhibited Cl^- current (insensitivity to dithiothreitol and 1–2 ps unitary conductance [12]). Another candidate-channel family is the bestrophins. For examination of this possibility, HEK cells were transfected with hBEST1 as previously described [16] and whole-cell Cl^- current was recorded by patch-clamp analysis. The intracellular solution contained 125–150 nM $[Ca^{2+}]_{free}$ and 2 mM Mg-ATP, sufficient to provide 50%–75% of maximal channel activation [16]. Whole-cell current was unaffected when 10 μM Ins(3,4,5,6)P_4 was perfused into the cell (Hartzell, Yu, and Shears, data not shown). Moreover, the Cl^- currents carried by bestrophins exhibited a near-linear relationship between current and voltage (data not shown, [4]), in contrast to the outward rectification that typifies Ins(3,4,5,6)P_4-regulated Cl^- currents [12, 14].

We then turned our attention to the ClC family. These are proteins that are often predominantly intracellular, but at least one of them, ClC-3, is also located in the plasma membrane [17]. HEK293-tsA201 cells (a popular cell line for ion-channel-expression studies) were transfected with ClC-3; electrophysiological analysis of the $tsA^{ClC\text{-}3}$ cells revealed a strongly outwardly rectifying Cl^- current (Figure 1A), in agreement with previous studies of ClC-3 [18], as well as of ClC-4 and ClC-5 [19]. When CaMKII was perfused into the cell through the patch pipette, whole-cell current increased > 10-fold within 10–20 min (Figure 1A); the delay reflects the small diffusion coefficient of large molecules, as well as the significant diffusional barrier imposed by the pipette tip [20]. Another consequence of CaMKII addition was that the relationship between current and voltage became more linear, thereby reducing the strength of the outward rectification (Figure 1A). CaMKII did not affect Cl^- currents in tsA cells in which ClC-3 was not overexpressed (data not shown, [21]). The addition of Ins(3,4,5,6)P_4 to the pipette solution prevented CaMKII from activating the ClC-3-dependent Cl^- current (Figures 1B and 1C). Both the potency of Ins(3,4,5,6)P_4 (IC_{50} = 4.6 μM; Figure 1D) and its specificity of action (neither Ins(1,3,4,5,6)P_5 nor Ins(1,4,5,6)P_4 affected Cl^- current; Figures 1B and 1C) are defining characteristics of the action of Ins(3,4,5,6)P_4 upon native CaMKII-activated Cl^- current [14]. The inhibition of native current by Ins(3,4,5,6)P_4 also has the distinctive feature of being attenuated by okadaic acid [12]. A similar pharmacological effect was observed in $tsA^{ClC\text{-}3}$ cells (Figure 1E). This is the first demonstration of a physiologically relevant and specific effect of Ins(3,4,5,6)P_4 upon a defined Cl^- channel in intact cells. In particular, the inhibition by Ins(3,4,5,6)P_4 of inward Cl^- current (Figures 1B and 1C), which by convention represents Cl^- efflux from the cell, recapitulates previous demonstrations of physiologically relevant inhibition by Ins(3,4,5,6)P_4 of Cl^- secretion from secretory epithelial cells [1, 13].

*Correspondence: shears@niehs.nih.gov

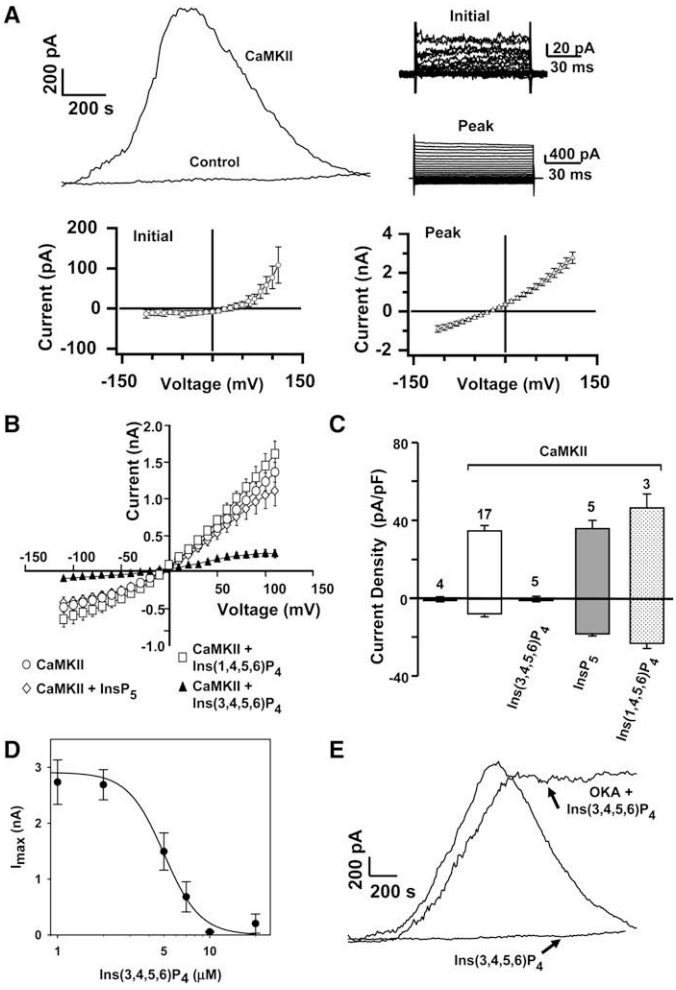

Figure 1. Electrophysiological Analysis of the Inhibition of CaMKII-Activated Cl^- Current by Ins(3,4,5,6)P_4 in tsA^{ClC-3} Cells

(A) Representative whole-cell currents from tsA^{ClC-3} cells in which autonomous CaMKII (20 μg/ml) was included in the pipette solution. Upper left panel: Representative time-course of current elicited during depolarizing voltage pulses to 110 mV from a holding potential of −40 mV every 10 s. Upper right panel: Families of currents recorded at the initiation ("initial") and peak of CaMKII-mediated current activation, during hyperpolarizing and depolarizing voltage pulses from a holding potential of −40 mV to potentials between −110 and 110 mV at 10 mV intervals. Lower panels: Average relationship between current and voltage from seven cells.

(B–E) Analysis of whole-cell current responses to 100 μM Ins(1,3,4,5,6)P_5, 100 μM Ins(1,4,5,6)P_4, or 10 μM (unless otherwise indicated) Ins(3,4,5,6)P_4. (B) Average relationship between current and voltage for current families elicited as in (A). (C) Mean current densities determined at 110 mV and −110 mV, with cell numbers indicated above each bar. (D) Effect of Ins(3,4,5,6)P4 concentration upon CaMKII-activated current (n = 3-6). Data are fitted to a single-site binding curve. (E) Representative time course of current activation by CaMKII (peak current = 3.18 ± 0.34 nA, n = 7) plus (in the pipette solution) either 10 μM Ins(3,4,5,6)P_4 + 100 nM okadaic acid ("OKA") (peak current = 2.64 ± 0.68 nA, n = 3) or 10 μM Ins(3,4,5,6)P_4 alone.

In panels that contain error bars, these represent standard errors of the mean.

Next, we investigated whether Ins(3,4,5,6)P_4 regulates ClC-3 in other biological contexts. In addition to being present in the plasma membrane, ClC-3 is well documented as localizing in the transferrin-positive endosomal compartment [17, 22–24] along with ClC-4 and ClC-5 [25, 26]. It has been proposed that Cl^- influx into the endosomes through ClCs provides the charge neutralization without which the electrogenic H^+-ATPase would not be capable of acidifying the vesicle interior [6, 24, 27]. A recent complication for the latter hypothesis is the determination that ClC-4 and ClC-5 are actually nCl^-/H^+ antiporters (n > 1) [28, 29]. This development does not oblige ClC-3 to function exclusively as a transporter rather than as a channel [30]. Functional switching between the two modes is also a possibility, perhaps mediated by CaMKII-dependent phosphorylation (Figure 1) or by the association of regulatory proteins [31]. Even in the event of nCl^-/H^+ antiport driven by vesicular ClC-3, its asymmetrical stoichiometry would still provide the necessary electrogenic support for luminal acidification [6]. Nevertheless, charge neutralization by nCl^-/H^+ antiport is clearly less energetically efficient than Cl^- influx [18]. Moreover, the outward rectification of ClCs has been argued to favor the opposite direction for Cl^- flux; namely, out of the endosome and into the cytoplasm [18]. This proposed Cl^- exit could then be coupled to H^+ influx into the endosome, thereby still facilitating luminal acidification [18]. The electrochemical driving force for this ion exchange could arise from the high intravesicular [Cl^-] that originates from the extracellular fluid that is inevitably trapped inside endosomes during their formation at the plasma membrane. Irrespective of the mechanisms involved, there is no doubt that ClCs contribute to endosomal acidification [6]. Thus, we recorded endosomal pH as an in situ biosensor for the regulation of ClC activity by Ins(3,4,5,6)P_4.

For these experiments, we chose baby hamster kidney (BHK) cells in which endogenous ClC-3 expression was below detectable levels (Figure 2A). We generated a new BHK cell line in which ClC-3 was stably transfected. Western-blot analysis of the BHK^{ClC-3} cell extracts revealed a band of 125–130 kDa (Figure 2A), representing the fully glycosylated mature protein. A smaller band of approximately 90 kDa may be immature ClC-3 (Figure 2A). Confocal immunofluorescence analysis revealed an intracellular, punctate distribution of ClC-3 (Figure 2A), indicating that it was localized in endosomes that were largely vesicular in nature. Next, the endocytic compartment in BHK cells was preloaded with the pH-sensitive fluorophore FITC conjugated to transferrin. Transferrin-positive endosomes have both tubulovesicular and morphologically distinct, punctate (globular) elements [32]. The latter subcompartment was the focus of our experiments, because exogenously expressed endosomal ClC-3 also showed a punctate distribution (Figure 2A). Typical examples of this relatively homogeneous population of punctate transferrin signals (103 ± 3 pixels) are highlighted by yellow arrows in Figure 2B. Luminal pH was determined in situ by fluorescence-ratio imaging of endosomes from single cells (Figure 2B and [25]). We employed a ratiometric analysis to compensate for any organelle-to-organelle variation in the luminal concentration of FITC-transferrin. The fluorophore signal was calibrated by equilibration of cells with buffers of known pH values containing ionophores so as to dissipate intracellular pH gradients (Figures 2B and 2C). The fluorescence ratio varied linearly with pH within the range 5.7–7.3 (r = 0.992).

In intact cells, [Ins(3,4,5,6)P_4] can be experimentally elevated by overexpression of ITPK1, but the multifunctional nature of this enzyme [10] causes accompanying changes in the levels of many additional inositol phosphates [33]. Instead,

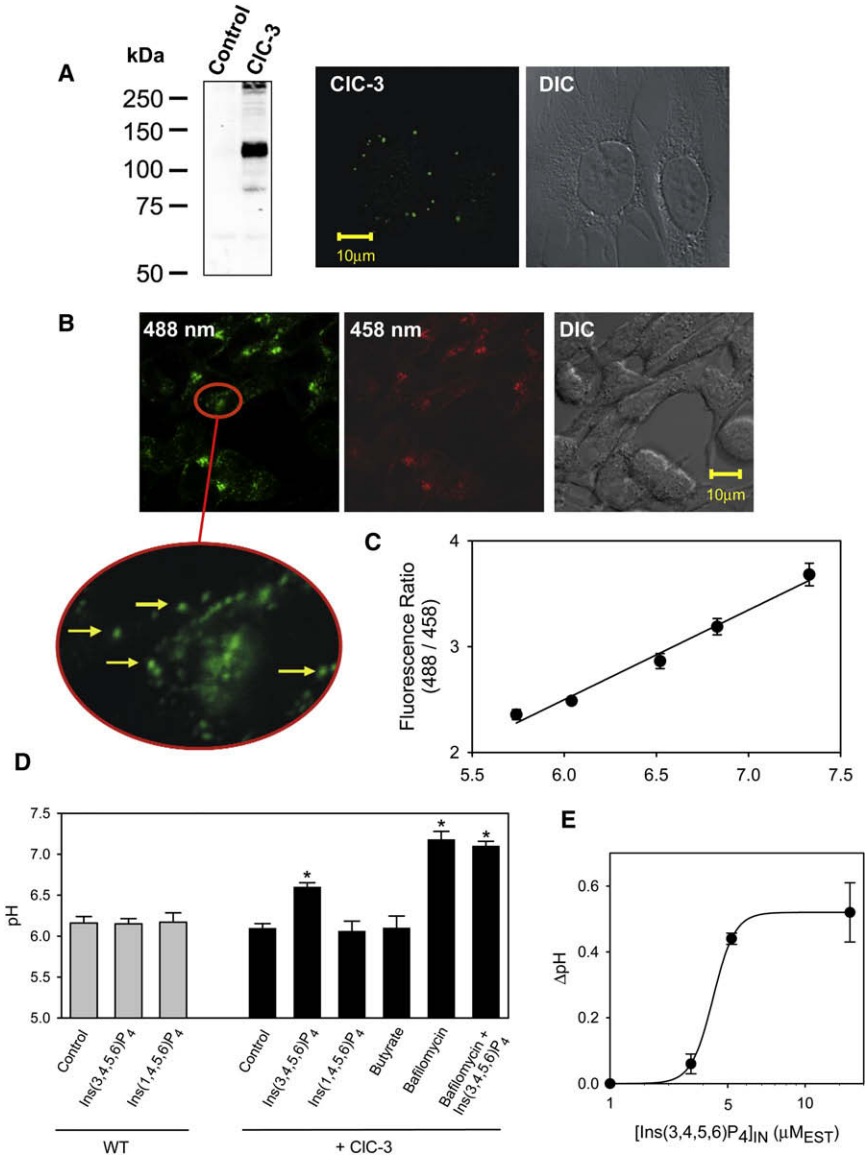

Figure 2. $Ins(3,4,5,6)P_4$ Regulates Endosomal Acidification by Inhibiting ClC-3

(A) Lysates of BHK cells (control) or $BHK^{ClC\text{-}3}$ cells were separated by 7% SDS-PAGE and transferred to nitrocellulose, and ClC-3 was detected with a murine monoclonal antibody. The same antibody was used for detection of ClC-3 in methanol-fixed cells via immunofluorescence microscopy (see Experimental Procedures).

(B) WT BHK cells or $BHK^{ClC\text{-}3}$ cells were each allowed to endocytose FITC-transferrin at 37°C. For calibration purposes, cells were equilibrated in buffers of known pH containing ionophores, followed by fluorescence-ratio imaging. An example (for $BHK^{ClC\text{-}3}$ cells at pH 7.3) is shown in (B), and for clarity of presentation (but not during data analysis), the brightness and contrast were increased by 30% with Microsoft Powerpoint. One cell is magnified and annotated with yellow arrows to highlight the regions that were defined as vesicular early endosomes and selected for pH analysis [32].

(C) A representative calibration plot is shown.

(D) Endosomal pH in cells that were treated either for 30 min with 0.5 μM bafilomycin or for 1 hr with 100 μM Bt_2-$Ins(3,4,5,6)P_4$/PM, 100 μM Bt_2-$Ins(1,4,5,6)P_4$/PM, or 200 μM butyrate (Bt). Data are from 3–6 experiments. Asterisks indicate $p < 0.001$ versus control.

(E) Cells were treated for 1 hr with 0, 10, 20, or 100 μM Bt_2-$Ins(3,4,5,6)P_4$/PM. The data (n = 3–4) show the relationship between ΔpH and the estimated (EST) intracellular concentration of $Ins(3,4,5,6)P_4$, based upon a delivery efficiency ($[Ins(3,4,5,6)P_4]_{IN}$ / $[Bt_2\text{-}Ins(3,4,5,6)P_4/PM]_{OUT}$) of 16% [13, 34] and assuming 1 μM $Ins(3,4,5,6)P_4$ in resting cells [13].

In panels that contain error bars, these represent standard errors of the mean.

so as to specifically study the effects of $Ins(3,4,5,6)P_4$, we used a cell-permeant, bioactivatable analog, Bt_2-$Ins(3,4,5,6)P_4$/PM [34]. This procedure did not affect endosomal pH in wild-type (WT) BHK cells (Figure 2D). Thus, in these cells, endogenous endosomal Cl^- channels were not substantially regulated by $Ins(3,4,5,6)P_4$. In contrast, in $BHK^{ClC\text{-}3}$ cells, treatment with cell-permeant $Ins(3,4,5,6)P_4$ led to significant alkalization of endosomal pH (0.5 pH units; Figure 2D). An IC_{50} value of 4.5 μM was obtained (Figure 2E), similar to the potency of $Ins(3,4,5,6)P_4$ action upon ClC in the plasma membrane (Figure 1D). In control experiments, we treated cells with bafilomycin, an H^+-ATPase inhibitor, and this elevated pH (Figure 2D). Given that endosomal Cl^- flux is electrogenically linked to the H^+-ATPase [6], we posited that inhibition of the ATPase should prevent $Ins(3,4,5,6)P_4$ from having any additional effect upon luminal pH. This was the result that we obtained (Figure 2D). Cell-permeant $Ins(1,4,5,6)P_4$ was an important negative control for specificity that had no effect upon endosomal pH (Figure 2D). The observation that $Ins(3,4,5,6)P_4$ caused endosomal pH to rise in the $BHK^{ClC\text{-}3}$ cells but not in WT BHK cells (Figure 2D) is valuable confirmation that ClC-3 contributes to vesicle acidification. Endosomal ClC-3 must now be considered a regulated signaling entity rather than merely subservient to vesicle acidification. The occurrence of this regulatory process in endosomes has additional significance; the endosomal compartment is a cell-signaling nexus from which emerges many of the spatiotemporal properties of certain biological messengers [35]; our data add an inositol phosphate to this complex, multifactorial paradigm.

Our results (Figure 2D) indicate that the endogenous Cl^- channels and/or transporters that are insensitive to $Ins(3,4,5,6)P_4$ in WT BHK cells are unable to compensate for inhibition of exogenous ClC-3 in the $BHK^{ClC\text{-}3}$ cells. This might simply reflect inherent kinetic differences between ClC isoforms, although it is also possible that overexpression of ClC-3 leads to a decrease in endosomal expression of endogenous Cl^- transporters.

Are other members of the ClC family regulated by $Ins(3,4,5,6)P_4$? There is no evidence for this in WT BHK cells, in which $Ins(3,4,5,6)P_4$ had no effect upon the endosomal pH set by endogenous Cl^- transporters (Figure 2D). In order to further study this idea, we utilized Caco-2 cells, for two reasons. First, they express very little ClC-3 protein [22, 27]. Second, previous work with these cells [25] has revealed that endosomal pH is set by endogenous heterodimers of ClC-4 and ClC-5, such that inhibition of either protein alone is sufficient to promote endosomal alkalosis. We again used FITC-transferrin to record

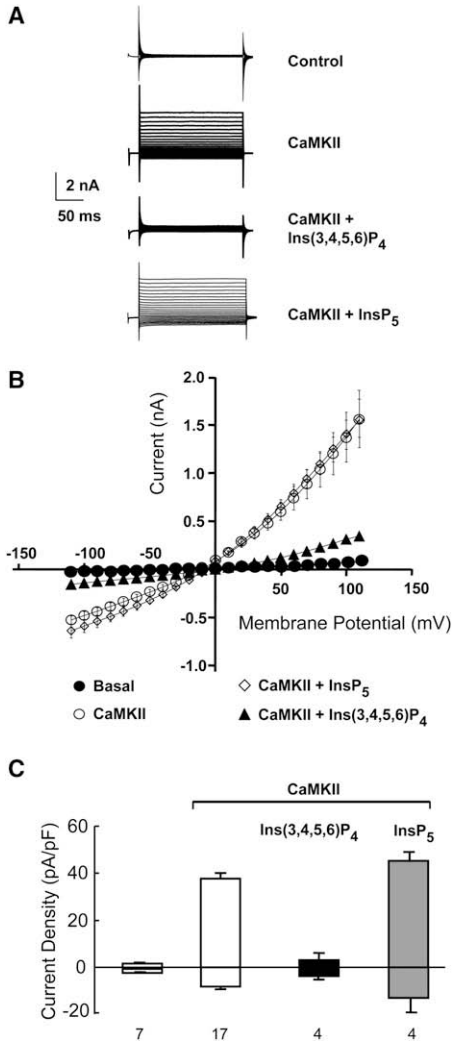

Figure 3. CaMKII-Activated ClC-3 Current Is Inhibited by Ins(3,4,5,6)P_4 in Cultured Rat P5 Hippocampal Neurons

Whole-cell currents were obtained, as described in Figure 1, from cultured hippocampal neurons in which autonomous CaMKII (20 μg/ml) was included in the pipette solution for 25 min plus, where indicated, either 10 μM Ins(3,4,5,6)P_4 or 100 μM Ins(1,3,4,5,6)P_5.

(A) Families of currents recorded during hyperpolarizing and depolarizing voltage pulses.

(B) Relationship between current and voltage.

(C) Average current densities at 110 mV and −110mV, with cell numbers indicated below each bar.

In panels that contain error bars, these represent standard errors of the mean.

endosomal pH. The value that we obtained (6.17 ± 0.08; n = 15) was unchanged (6.12 ± 0.13; n = 3) by 2 hr treatment with 100 μM Bt_2-Ins(3,4,5,6)P_4/PM. Therefore, we conclude that Ins(3,4,5,6)P_4 does not significantly regulate endosomal pH through an interaction with either ClC-4 or ClC-5.

We next studied the influence of Ins(3,4,5,6)P_4 upon plasma membrane Cl^- current in another context; namely, neonatal hippocampal neurones. This particular endogenous Cl^- current has conclusively been attributed to ClC-3, because it is absent from clc-$3^{-/-}$ mice [31]. The unitary conductance of this ClC-dependent Cl^- current is relatively low (3 pS), and two-pore ("double-barreled") behavior was observed [31]; both of these characteristics are distinguishing properties of the ClC family [6]. The introduction of CaMKII into hippocampal neurones dramatically activated a whole-cell Cl^- current that displayed outward rectification (Figure 3), similar to the CaMKII-activated, ClC-3-mediated Cl^- current in tsA cells (Figure 1). When we perfused Ins(3,4,5,6)P_4 into the neuronal cells, the CaMKII-activated Cl^- current was almost completely inhibited (Figure 3). In control experiments, Ins(1,3,4,5,6)P_5 did not affect Cl^- current (Figure 3). This specific regulation of Cl^- fluxes by Ins(3,4,5,6)P_4 is likely to have regulatory significance; an interplay between the degree of activation of ClC-3 and NMDA receptors may control the synaptic efficacy in generating action potentials [31]. Long-term changes in synaptic efficacy are thought to form a cellular basis for information storage and memory formation. Thus, Ins(3,4,5,6)P_4 is a molecule that has the potential to affect neuronal development, through its ability to regulate ClC-3 activity.

ClC-3 has many other roles, including tumor cell migration [7], bone remodeling [36], apoptosis [8], and inflammatory responses [9]. We can now anticipate that Ins(3,4,5,6)P_4 might also regulate these processes. Overall, our study shows that Ins(3,4,5,6)P_4 is an intracellular signal with a far greater biological repertoire than has previously been appreciated. The knowledge that ClC-3 function is regulated by Ins(3,4,5,6)P_4 is also a substantial experimental advance, because it offers new opportunities for determining the mechanism of action of this inositol phosphate.

Experimental Procedures

Cell Culture

Caco-2 cells were cultured in DMEM:F12 (GIBCO no.11330) with 10% FBS (Hyclone) and 5% CO_2. BHK-21 cells were grown in DMEM/F12, 5% FBS at 37°C in 5%CO_2. These cells were stably transfected with human ClC-3 (also known as "long-ClC-3A"; GenBank accession no. NP_001820) in pcDNA3 and pNUT vector with the use of Lipofectamine Plus (Invitrogen). $BHK^{ClC\text{-}3}$ cells were selected with the use of 500 μM methotrexate in the growth medium. The ClC-3 cDNA was also subcloned in the pcDNA3.1 zeo^+ vector (Invitrogen, CA) and was transfected into tsA cells with SuperFect reagent (QIAGEN, CA) (see [21] for details). The $tsA^{ClC\text{-}3}$ cells were selected with zeocin (Invitrogen) at 400 μg/ml and maintained at 200 μg/ml. P5 hippocampal neuronal cultures were obtained as previously described [31].

Endosomal pH Measurements

The endosomal pH of Caco-2 and BHK cells was determined through fluorescence-ratio imaging of FITC-transferrin [25]. Cells plated on glass bottom coverslip dishes (MatTek, Ashland, MA) were allowed to reach 90% confluency and were serum-starved for 2 hr. Endosomes were identified by incubation of cells for 20–180 min at 37°C with 200 μg/ml FITC-transferrin (Invitrogen) in medium containing 140 mM NaCl, 5 mM KCl, 5 mM glucose, 1 mM $CaCl_2$, 1 mM $MgCl_2$, 10 mM HEPES, pH 7.4 (endosomal pH was independent of the time of incubation with FITC-transferrin). Cells were incubated at 37°C with either 0.5 μM bafilomycin (30 min; dissolved in methanol), vehicle, or cell-permeant Bt_2-Ins(3,4,5,6)P_4/PM or Bt_2-Ins(1,4,5,6)P_4/PM (SiChem, Bremen, Germany) for 2 hr. The vehicle for the inositol phosphate analogs was a mixture of anhydrous methyl sulfoxide (Sigma) and pluronic (final concentrations 0.36% and 0.02%, respectively).

For removal of surface-bound FITC-transferrin, cells were washed three times at 37°C with phosphate-buffered saline (pH 5.0). Cells were imaged with a PlanApo 63×/1.4 Oil DIC63X objective on an LSM 510 meta-NLO mounted on an Axiovert 100M microscope and acquired with the Carl Zeiss LSM 510 software v.3.2 SP2 (Carl Zeiss, Thornwood, NY). Pixel width was set to 0.07 μm, and a pinhole setting of 1 Airy unit was used. The focal plane was then adjusted to acquire images from the center of the cells. FITC-transferrin was visualized by acquiring sequential images with the use of excitation wavelengths of 488 nm and then 458 nm, while the emission signal was consistently collected with a 505 nm low-pass filter. Each dual-excitation image pair was imported into the MetaFluor Offline software, v.6.3r6 (Molecular Devices, Downingtown, PA), where approximately 10–12 endosomes from 3–4 cells were classified as regions of interest (ROI) by manual definition of a circle (103 ± 3 pixels) around a vesicular endosome. The

fluorescence ratio was determined from each ROI as the average pixel intensity taken from the emission signal at 488 nm excitation (pH dependent) and divided by the emission signal collected when 458 nm excitation (pH independent) was used. In cases when the intensity of a given ROI was low, we performed a background subtraction, the value of which was defined from an equivalently sized "ROI" placed outside the cell. The data derived by the MetaFluor software were then exported to Microsoft Excel. The relationship between fluorescence ratio and pH was determined by equilibration of cells in a series of standards (in which the pH was adjusted from 5.7 to 7.3) with the use of the following medium: 140 mM KCl, 10 mM NaCl, 10 mM HEPES, 5 mM glucose, 1 mM $CaCl_2$, 1 mM $MgCl_2$, 20 μM monensin, and 20 μM nigericin.

Immunofluorescence Microscopy

BHK-21 cells were fixed in MeOH (−20°C) for 10 min, permeabilized with 0.1% Saponin in PBS (4°C, 60 min), and blocked with 5% goat serum, 1% BSA in PBS. Mouse monoclonal antibody 34.1 [22] was applied at a concentration of 3 mg/ml followed by goat anti-mouse Alexa Fluor 488 IgG conjugate (2.5 mg/ml) for detection of ClC-3. Cells were imaged with a Plan-Apochromat 63×/NA:1.4 Oil DIC objective on a Zeiss LSM 510 confocal laser-scanning microscope. Excitation was at 488 nm via an Argon Laser, a BP505-530 filter was employed for emission. DIC, and fluorescence images were obtained simultaneously. The pinhole setting was 1 Airy unit.

Electrophysiology

All patch-clamp recordings were made with quartz pipettes and an EPC-9 amplifier (HEKA Elektronik, Lambrecht[Pfalz], Germany). Extra- and intracellular solutions were designed such that Cl^- was the primary charge carrier. The bath solution contained: 140 mM HCl, 140 mM methyl D-glucamine, 2 mM $CaCl_2$, 1 mM $MgCl_2$, and 10 mM HEPES pH 7.4. The pipette solution contained 40 mM HCl, 100 mM L-glutamic acid, 140 mM methyl D-glucamine, 0.2 mM $CaCl_2$, 2 mM $MgCl_2$, 1 mM EGTA, 10 mM HEPES, pH 7.2, and 2 mM ATP-Mg. Free Ca^{2+} was calculated to be 40 nM. Ca^{2+}-independent, autonomously active, autophosphorylated CaMKII was prepared daily [21] and was introduced into the cell via the patch pipette. The Cl^- equilibrium potential was calculated to be −31 mV . Under these ionic conditions, nonspecific leak current was identified as a depolarizing shift in reversal potential. Currents were elicited through a series of test pulses from −110 to 110 mV in 10 mV increments from a holding potential of −40 mV. Test pulses (200 ms) were delivered at 2 s intervals. Current recordings were acquired at 2 kHz and filtered at 1 kHz.

Acknowledgments

We are grateful to Jeff Tucker for assistance with the confocal imaging. This research was supported by the Intramural Research Program of the National Institutes of Health (NIH) at the National Institute of Environmental Health Sciences, by an NIH grant supporting M.G. (P50 HL60280), and by the following grants to D.J.N: NIH R01 GM36823, NIH R56 DK080364, and Nelson07G0 awarded by the Cystic Fibrosis Foundation.

Received: May 28, 2008
Revised: August 8, 2008
Accepted: August 28, 2008
Published online: October 23, 2008

References

1. Yang, L., Reece, J., Gabriel, S.E., and Shears, S.B. (2006). Apical localization of ITPK1 enhances its ability to be a modifier gene product in a murine tracheal cell model of cystic fibrosis. J. Cell Sci. *119*, 1320–1328.
2. Menniti, F.S., Oliver, K.G., Putney, J.W., Jr., and Shears, S.B. (1993). Inositol phosphates and cell signalling: New views of InsP5 and InsP6. Trends Biochem. Sci. *18*, 53–56.
3. Eggermont, J. (2004). Calcium-activated chloride channels: (un)known, (un)loved? Proc. Am. Thorac. Soc. *1*, 22–27.
4. Pusch, M. (2004). Ca(2+)-activated chloride channels go molecular. J. Gen. Physiol. *123*, 323–325.
5. Kunzelmann, K., Milenkovic, V.M., Spitzner, M., Soria, R.B., and Schreiber, R. (2007). Calcium-dependent chloride conductance in epithelia: is there a contribution by Bestrophin? Pflugers Arch. *454*, 879–889.
6. Jentsch, T.J. (2008). CLC chloride channels and transporters: from genes to protein structure, pathology and physiology. Crit. Rev. Biochem. Mol. Biol. *43*, 3–36.
7. Mao, J., Chen, L., Xu, B., Wang, L., Li, H., Guo, J., Li, W., Nie, S., Jacob, T.J., and Wang, L. (2008). Suppression of ClC-3 channel expression reduces migration of nasopharyngeal carcinoma cells. Biochem. Pharmacol. *75*, 1706–1716.
8. Claud, E.C., Lu, J., Wang, X.Q., Abe, M., Petrof, E.O., Sun, J., Nelson, D.J., Marks, J.D., and Jilling, T. (2008). Platelet-activating Factor induced chloride channel activation is associated with intracellular acidosis and apoptosis of intestinal epithelial cells. Am. J. Physiol. Gastrointest. Liver Physiol. *294*, G1191–G1200.
9. Moreland, J.G., Davis, A.P., Bailey, G., Nauseef, W.M., and Lamb, F.S. (2006). Anion channels, including ClC-3, are required for normal neutrophil oxidative function, phagocytosis, and transendothelial migration. J. Biol. Chem. *281*, 12277–12288.
10. Chamberlain, P.P., Qian, X., Stiles, A.R., Cho, J., Jones, D.H., Lesley, S.A., Grabau, E.A., Shears, S.B., and Spraggon, G. (2007). Integration of inositol phosphate signaling pathways via human ITPK1. J. Biol. Chem. *282*, 28117–28125.
11. Ho, M.W.Y., and Shears, S.B. (2002). Regulation of calcium-activated chloride channels by inositol 3,4,5,6-tetrakisphosphate. In Current Topics in Membranes, **53**, C.M. Fuller, ed. (London: Academic Press), pp. 345–363.
12. Ho, M.W.Y., Kaetzel, M.A., Armstrong, D.L., and Shears, S.B. (2001). Regulation of a Human Chloride Channel: A Paradigm for Integrating Input from Calcium, CaMKII and Ins(3,4,5,6)P_4. J. Biol. Chem. *276*, 18673–18680.
13. Vajanaphanich, M., Schultz, C., Rudolf, M.T., Wasserman, M., Enyedi, P., Craxton, A., Shears, S.B., Tsien, R.Y., Barrett, K.E., and Traynor-Kaplan, A.E. (1994). Long-term uncoupling of chloride secretion from intracellular calcium levels by Ins(3,4,5,6)P_4. Nature *371*, 711–714.
14. Xie, W., Kaetzel, M.A., Bruzik, K.S., Dedman, J.R., Shears, S.B., and Nelson, D.J. (1996). Inositol 3,4,5,6-tetrakisphosphate inhibits the calmodulin-dependent protein kinase II-activated chloride conductance inT84 colonic epithelial cells. J. Biol. Chem. *271*, 14092–14097.
15. Fuller, C.M., Kovacs, G., Anderson, S.J., and Benos, D.J. (2005). The CLCAs: Proteins with ion chanel, cell adhesion and tumor suppressor functions. In Defects of secretion in cystic fibrosis, C. Schultz, ed. (New York: Springer), pp. 83–102.
16. Yu, K., Cui, Y., and Hartzell, H.C. (2006). The bestrophin mutation A243V, linked to adult-onset vitelliform macular dystrophy, impairs its chloride channel function. Invest. Ophthalmol. Vis. Sci. *47*, 4956–4961.
17. Zhao, Z., Li, X., Hao, J., Winston, J.H., and Weinman, S.A. (2007). The ClC-3 chloride transport protein traffics through the plasma membrane via interaction of an N-terminal dileucine cluster with clathrin. J. Biol. Chem. *282*, 29022–29031.
18. Matsuda, J.J., Filali, M.S., Volk, K.A., Collins, M.M., Moreland, J.G., and Lamb, F.S. (2008). Overexpression of CLC-3 in HEK293T cells yields novel currents that are pH dependent. Am. J. Physiol. Cell Physiol. *294*, C251–C262.
19. Friedrich, T., Breiderhoff, T., and Jentsch, T.J. (1999). Mutational analysis demonstrates that ClC-4 and ClC-5 directly mediate plasma membrane currents. J. Biol. Chem. *274*, 896–902.
20. Pusch, M., and Neher, E. (1988). Rates of diffusional exchange between small cells and a measuring patch pipette. Pflugers Arch. *411*, 204–211.
21. Robinson, N.C., Huang, P., Kaetzel, M.A., Lamb, F.S., and Nelson, D.J. (2004). Identification of an N-terminal amino acid of the CLC-3 chloride channel critical in phosphorylation-dependent activation of a CaMKII-activated chloride current. J. Physiol. *556*, 353–368.
22. Gentzsch, M., Cui, L., Mengos, A., Chang, X.B., Chen, J.H., and Riordan, J.R. (2003). The PDZ-binding chloride channel ClC-3B localizes to the Golgi and associates with cystic fibrosis transmembrane conductance regulator-interacting PDZ proteins. J. Biol. Chem. *278*, 6440–6449.
23. Stobrawa, S.M., Breiderhoff, T., Takamori, S., Engel, D., Schweizer, M., Zdebik, A.A., Bösl, M.R., Ruether, K., Jahn, H., Draguhn, A., et al. (2001). Disruption of ClC-3, a chloride channel expressed on synaptic vesicles, leads to a loss of hippocampus. Neuron *29*, 185–196.
24. Hara-Chikuma, M., Yang, B., Sonawane, N.D., Sasaki, S., Uchida, S., and Verkman, A.S. (2005). ClC-3 chloride channels facilitate endosomal acidification and chloride accumulation. J. Biol. Chem. *280*, 1241–1247.
25. Mohammad-Panah, R., Harrison, R., Dhani, S., Ackerley, C., Huan, L.J., Wang, Y.C., and Bear, C.E. (2003). The chloride channel ClC-4

contributes to endosomal acidification and trafficking. J. Biol. Chem. *278*, 29267–29277.
26. Suzuki, T., Rai, T., Hayama, A., Sohara, E., Suda, S., Itoh, T., Sasaki, S., and Uchida, S. (2006). Intracellular localization of ClC chloride channels and their ability to form hetero-oligomers. J. Cell. Physiol. *206*, 792–798.
27. Weylandt, K.H., Nebrig, M., Jansen-Rosseck, N., Amey, J.S., Carmena, D., Wiedenmann, B., Higgins, C.F., and Sardini, A. (2007). ClC-3 expression enhances etoposide resistance by increasing acidification of the late endocytic compartment. Mol. Cancer Ther. *6*, 979–986.
28. Picollo, A., and Pusch, M. (2005). Chloride/proton antiporter activity of mammalian CLC proteins ClC-4 and ClC-5. Nature *436*, 420–423.
29. Scheel, O., Zdebik, A.A., Lourdel, S., and Jentsch, T.J. (2005). Voltage-dependent electrogenic chloride/proton exchange by endosomal CLC proteins. Nature *436*, 424–427.
30. Lisal, J., and Maduke, M. (2008). The ClC-0 chloride channel is a 'broken' Cl(-)/H(+) antiporter. Nat. Struct. Mol. Biol. *15*, 805–810.
31. Wang, X.Q., Deriy, L.V., Foss, S., Huang, P., Lamb, F.S., Kaetzel, M.A., Bindokas, V., Marks, J.D., and Nelson, D.J. (2006). CLC-3 Channels Modulate Excitatory Synaptic Transmission in Hippocampal Neurons. Neuron *52*, 321–333.
32. Mayor, S., Presley, J.F., and Maxfield, F.R. (1993). Sorting of membrane components from endosomes and subsequent recycling to the cell surface occurs by a bulk flow process. J. Cell Biol. *121*, 1257–1269.
33. Verbsky, J.W., Chang, S.C., Wilson, M.P., Mochizuki, Y., and Majerus, P.W. (2005). The pathway for the production of inositol hexakisphosphate in human cells. J. Biol. Chem. *280*, 1911–1920.
34. Schultz, C. (2003). Prodrugs of biologically active phosphate esters. Bioorg. Med. Chem. *11*, 885–898.
35. von, Z.M., and Sorkin, A. (2007). Signaling on the endocytic pathway. Curr. Opin. Cell Biol. *19*, 436–445.
36. Okamoto, F., Kajiya, H., Toh, K., Uchida, S., Yoshikawa, M., Sasaki, S., Kido, M.A., Tanaka, T., and Okabe, K. (2008). Intracellular ClC-3 chloride channels promote bone resorption in vitro through organelle acidification in mouse osteoclasts. Am. J. Physiol. Cell Physiol. *294*, C693–C701.